annalen der physik
www.ann-phys.org

Possible Polarization Measurements in Elastic Scattering at the Gamma Factory Utilizing a 2D Sensitive Strip Detector as Dedicated Compton Polarimeter

Wilko Middents, Günter Weber, Uwe Spillmann, Thomas Krings, Marco Vockert, Andrey Volotka, Andrey Surzhykov, and Thomas Stöhlker*

For photon energies from several 10 keV up to a few MeV Compton polarimetry is an indispensable tool to gain insight into subtle details of fundamental atomic radiative processes. Within the SPARC collaboration several segmented semiconductor detectors are developed that are well suited for application as efficient Compton polarimeters. In this report, these recent developments are reviewed and it is discussed how Compton polarimetry can be employed at the upcoming Gamma Factory.

W. Middents, M. Vockert, Th. Stöhlker
Institute of Optics and Quantum Electronics
Friedrich Schiller University Jena
Max-Wien-Platz 1, Jena 07743, Germany
E-mail: wilko.middents@uni-jena.de

W. Middents, G. Weber, M. Vockert, Th. Stöhlker
Helmholtz Institute Jena
Fröbelstieg 3, Jena 07743, Germany

G. Weber, U. Spillmann, Th. Stöhlker
GSI Helmholtzzentrum für Schwerionenforschung GmbH
Planckstraße 1, Darmstadt 64291, Germany

T. Krings
Institut für Kernphysik
Forschungszentrum Jülich
Wilhelm-Johnen-Straße, Jülich 52425, Germany

A. Volotka
School of Physics and Engineering
ITMO University
Kronverskiy pr. 49, St. Petersburg 1979034, Russia

A. Surzhykov
Fundamental physics for metrology
Physikalisch Technische Bundesanstalt
Braunschweig D-38116, Germany

A. Surzhykov
Institut für Mathematische Physik
Technische Universität Braunschweig
Braunschweig D-38106, Germany

A. Surzhykov
Laboratory for Emerging Nanometrology Braunschweig
Braunschweig D-38106, Germany

The ORCID identification number(s) for the author(s) of this article can be found under https://doi.org/10.1002/andp.202100285

DOI: 10.1002/andp.202100285

1. Introduction

Photon polarimetry is an indispensable tool to gain insight into subtle details of the directionality of photon emission processes. This is in particular true in astrophysics where complementary information on the characteristics of the radiation, such as angular distributions, are not accessible.[1,2] But also in the laboratory it is desirable and often necessary to take into account the polarization characteristics of incoming and outgoing particles to provide the most rigorous tests of our theoretical understanding of the underlying processes. A lot of radiative processes, such as X-ray scattering,[3,4] ion–atom collisions[5] and radiative electron capture,[6] exhibit distinct polarization features, thus a complete measurement must also include the polarization analysis of the process. Moreover, it was recently shown that X-ray polarimetry can also be used as a tool for monitoring the polarization of particle beams, such as electrons[7] or ions.[8]

Possible ways to analyze the polarization characteristics of a photon beam highly depend on the energy regime. For low-energy photons in the IR to UV range standard polarimetry techniques using optical active media are well developed and applied since a long time. Moving to higher photon energies, in the soft to medium X-ray regime polarimetry techniques based on Bragg diffraction[9] are commonly used. However, when going to photon energies above several tens of keV all these techniques cease to be efficient. In this regime Compton scattering becomes the dominant polarization-sensitive interaction process, ranging up to a few MeV photon energy. Its sensitivity to the (linear) polarization of the incident radiation is due to the fact, that the scattered photon is preferentially emitted in the direction perpendicular to the incident photon's electric field vector, whereas emission in the parallel direction is less probable. Compton polarimetry is based on the analysis of the resulting anisotropy of the emission pattern of Compton scattered photons.

Within the Stored Particles Atomic Physics Research Collaboration (SPARC),[10,11] covering atomic physics at GSI and FAIR, several X-ray detectors were developed on the basis of large double-sided segmented semiconductor crystals that are well suited for the application as Compton polarimeters. In the recent years, these detectors enabled measurements of the polarization transfer in Rayleigh scattering[12] as well as in the

Bremsstrahlung process[7] as well as the polarization characteristics of photons emitted by radiative electron capture[6], and of characteristic transitions within highly charged, heavy ions.[13] Recently, a dedicated Si(Li) Compton polarimeter was commissioned that features a significantly improved energy resolution of about 1 keV at a photon energy of 60 keV.[14] In this work we will report on the aforementioned developments of the Compton polarimeters and discuss their possible application at the upcoming Gamma Factory.

2. Compton Polarimetry

Compton scattering, being the inelastic scattering of a photon on a free (or quasi–free) electron, can be described by the Klein–Nishina formula which gives the angular differential cross section of the process

$$\frac{\mathrm{d}\sigma}{\mathrm{d}\Omega}_{\mathrm{KN}}(\theta,\phi) = \frac{1}{2}r_0^2 \cdot \left(\frac{h\nu'}{h\nu}\right)^2 \cdot \left(\frac{h\nu'}{h\nu} + \frac{h\nu}{h\nu'} - 2\sin^2\theta\cos^2\phi\right) \quad (1)$$

Here r_0 is the classical electron radius, ν is the frequency of an incident photon and $\nu' = \nu'(\theta)$ is the frequency of the outgoing photon, scattered under the polar angle θ. The aforementioned anisotropy is given by the dependence on ϕ, being the azimuthal angle between the electrical field vector of the incident photon and the propagation direction of the scattered photon. This can be used to reconstruct the degree of linear polarization and the orientation of the polarization axis of a photon beam from the azimuthal emission pattern of Compton scattered photons, as first described by Metzger and Deutsch in 1950.[15] For an extensive overview of Compton polarimetry the reader is referred to the review by Lei, Dean, and Hills.[16]

During the last two decades, several segmented large-volume semiconductor detectors were developed as dedicated Compton polarimeters by the SPARC collaboration. One of these detectors is shown in **Figure 1**a. It consists of a lithium-diffused silicon crystal allowing an efficient use of the detector for photon energies up to 200 keV. The detector crystal (Figure 1b) has a thickness of 9 mm and an active area of 32 mm×32 mm which is segmented on front and back side into 32 strips of 1 mm width each with the strips on front and backside being oriented perpendicular to each other. This segmentation of the crystal, leading to an array of 1024 pseudo-pixels, makes it into a high-resolution position-sensitive detector. Each of these strips has its own readout electronics with a cooled preamplification stage leading to an energy resolution of less than 1 keV at a photon energy of 60 keV.[14] The detector crystal serves as Compton scatterer and detector for the scattered photons at the same time. This "monolithic" polarimeter design is much more efficient compared to former polarimeter setups where individual detectors are used as a scatterer and an absorber and typically only a small fraction of the complete azimuthal scattering distribution is covered. If an incident photon is Compton scattered inside the detector crystal and the scattered photon is absorbed inside the crystal as well, information about time, energy and position of both interactions can be used to reconstruct the Compton event.[17] A typical reconstructed scattering profile can be seen in Figure 1c. Here the center of scattering was set to zero while the x–y profile shows the detected Compton scattered photons. From this reconstruction of the scattering events the azimuthal scattering profile, as shown in Figure 1d can be received in order to extract the degree of linear polarization and the orientation of the polarization vector.[18]

2.1. Example Application of the Compton Polarimeter: Polarization Measurements in Elastic Scattering of Hard X-Rays

Applying the Compton polarimeter in experimental studies allows in-depth tests of the polarization-dependent features in fundamental processes. One such fundamental process in which polarization studies will allow for more rigorous testing is the elastic scattering of hard X-rays by atoms.[3] Depending on the scattering partner, one can differentiate into separate processes. The scattering by bound electrons is referred to as Rayleigh scattering,[19] while nuclear Thomson scattering[20] and nuclear resonance scattering[21] describe elastic scattering involving the nucleus as scattering partner. Additionally Delbrück scattering describes the scattering of photons by vacuum fluctuations in the presence of a heavy nucleus.[22] The total scattering amplitude $A(\theta)$ depends on the angle θ between incident and scattered photon and is given by the coherent sum of individual amplitudes for each process

$$A(\theta) = A^{(\mathrm{R})}(\theta) + A^{(\mathrm{NT})}(\theta) + A^{(\mathrm{NR})}(\theta) + A^{(D)}(\theta) \quad (2)$$

For the scattering by a closed-shell target atom, the absolute value of the scattering amplitude $|A(\theta)|^2$ is resolvable into the components $|A(\theta)_\perp|^2$ and $|A(\theta)_\parallel|^2$ describing the parts of the scattered radiation being polarized perpendicular and parallel to the scattering plane, as spanned by the directions of incident and outgoing photons. These quantities can be accessed by state-of-the-art calculations using the S-matrix approach.[3] The (squares of the) amplitudes $A_\parallel$ and $A_\perp$ can be employed to calculate all the properties of the scattering process. Most naturally this can be done within the framework of the density matrix approach. Since the detailed discussion of the density matrix of incident and scattered radiation has been presented in the literature before, for example, refs. [23, 24], here we restrict ourselves just to the main expressions. For example, the angle–differential cross section of the scattering of incident light with the degree of linear polarization $P_{l,i}$ is given by

$$\frac{\mathrm{d}\sigma}{\mathrm{d}\Omega}(\theta,\varphi) = \frac{1}{4}\left[|A_\parallel(\theta)|^2 + |A_\perp(\theta)|^2\right] + \frac{1}{4}P_{l,i}\left[|A_\parallel(\theta)|^2 - |A_\perp(\theta)|^2\right]\cos(2\varphi) \quad (3)$$

with φ being the azimuthal scattering angle between the polarization plane of the incident beam and the scattering plane. The geometry of the described process of an initially linearly polarized photon beam being scattered on an atomic target explaining the used angles is shown in **Figure 2**.

The scattered beam will then be polarized with a certain degree of linear polarization $P_{l,f}$ under the polarization angle χ to the scattering plane. It makes sense to introduce the Stokes parameters $P_{1,f}$ and $P_{2,f}$ that are defined by the fractions of the intensities of the scattered beam polarized under different angles to the scattering plane

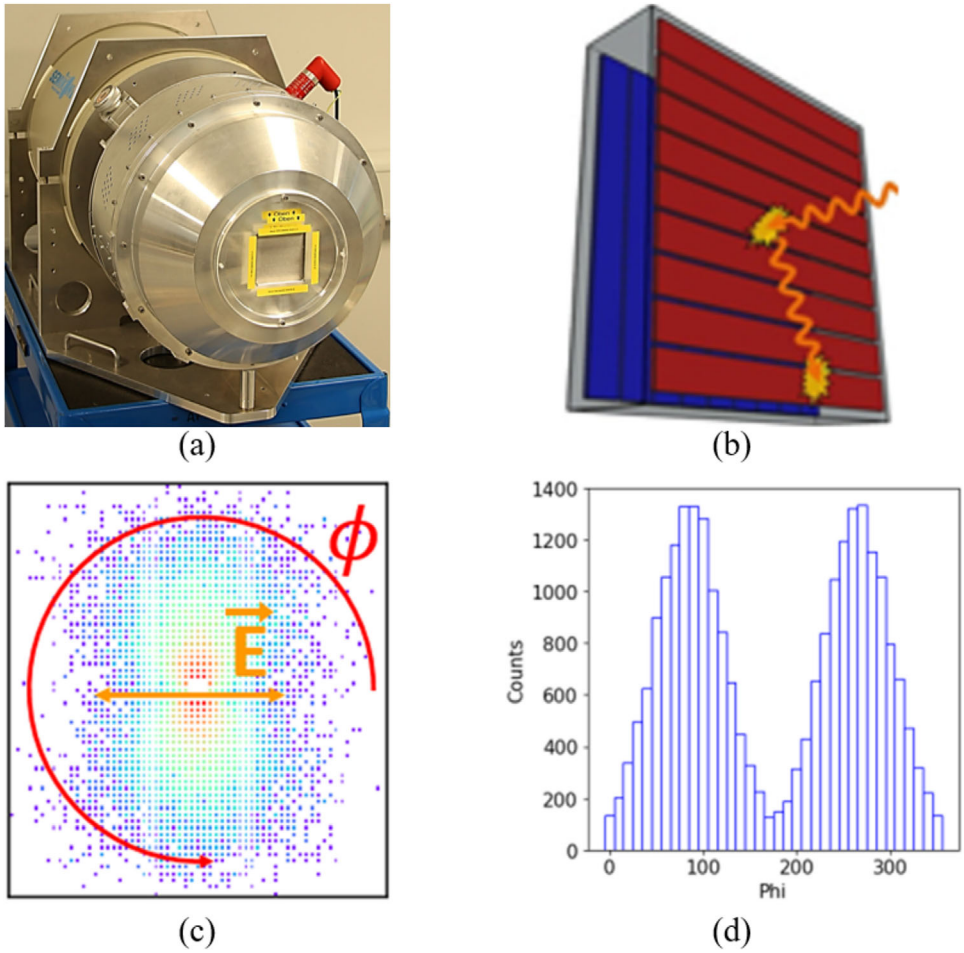

Figure 1. a) An image of the Compton polarimeter. b) Schematic principle of the detector crystal. The segmented crystal structure is shown. When an incident photon is Compton scattered on the detector, the scattered photon can as well be absorbed inside the detector. After a sufficient number of (scattering) events have accumulated, the angular distribution of scattered photons follows the Klein–Nishina formula. c) An example image of the Compton scattering distribution detected by the Compton polarimeter on the detector screen. The data set was generated by a Monte-Carlo simulation of the detector. The orientation of the polarization vector of the incident beam and the direction of the azimuthal scattering angle are shown as well. d) The azimuthal scattering profile of (c) where spurious effects due to the pixel geometry of the detector screen were avoided by normalizing the data to an isotropic distribution, meaning $P_L = 0$.

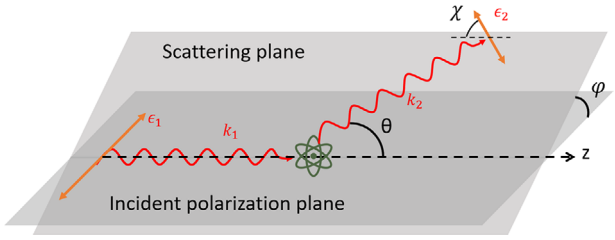

Figure 2. The geometry of elastic scattering of a linearly polarized incident photon beam on an atomic target. The polarization plane of the incident beam is spanned by the wave vector $\boldsymbol{k_1}$ and the polarization vector $\boldsymbol{\epsilon_1}$ of the incident beam. The scattered beam, spanning the scattering plane with the incident beam is defined by the polar scattering angle θ between the incident and scattered beam and the azimuthal scattering angle φ between the polarization plane of the incident beam and the scattering plane. The angle between the polarization vector of the scattered beam $\boldsymbol{\epsilon_2}$ and the scattering plane is the polarization angle χ.

$$P_{1,f} = \frac{I_0 - I_{90}}{I_0 + I_{90}} = P_{l,f}\cos(2\chi)$$
$$P_{2,f} = \frac{I_{45} - I_{135}}{I_{45} + I_{135}} = P_{l,f}\sin(2\chi) \tag{4}$$

Assuming no occurring circular polarization component, as is valid for most highly linearly polarized radiation sources, the Stokes parameters can be written in terms of the components of the scattering amplitude as[24]

$$P_{1,f} = \frac{|A_\parallel|^2 - |A_\perp|^2 + P_{l,i}\cos(2\varphi)\left[|A_\parallel|^2 + |A_\perp|^2\right]}{|A_\parallel|^2 + |A_\perp|^2 + P_{l,i}\cos(2\varphi)\left[|A_\parallel|^2 - |A_\perp|^2\right]}$$
$$P_{2,f} = \frac{2P_{l,i}\sin(2\varphi)Re\left(A_\parallel A_\perp^*\right)}{|A_\parallel|^2 + |A_\perp|^2 + P_{l,i}\cos(2\varphi)\left[|A_\parallel|^2 - |A_\perp|^2\right]} \tag{5}$$

For a complete characterization of the scattering process not only the scattering cross section is of interest but also the polarization characteristics need to be regarded. While the cross section measurement only gives the sum and difference of the absolute values of the scattering amplitudes, determining the Stokes parameters provides access to the real value of the (product of) scattering amplitudes. Thus a much more sensitive test of the theoretical models can be achieved.

For photon energies from a few keV to the MeV range Rayleigh scattering is the dominant component of elastic scattering while the other contributions being Delbrück scattering, nuclear Thomson scattering and giant dipole resonance scattering first become relevant at higher photon energies.[3] While polarization characteristics of Rayleigh scattering are theoretically studied in great detail,[24–27] for a long time polarized X-ray sources were not intense and polarimeters not efficient enough to perform an elastic scattering study in which both the polarization of the incident and the outgoing radiation are determined. Before the introduction of powerful sources of hard X-rays, such as the third-generation light-source PETRA III at DESY, incident polarized photon beams were produced from intense gamma sources whose radiation was polarized by scattering from a production target before it could be used in a scattering experiment as shown in Figure 1 of ref. [23]. The need to collimate the emitted photons to form a beam both at the point of initial emission from the gamma source as well as after the polarizer target results in low flux of the incident beam. Combined with the relatively low cross section of the elastic scattering process itself in combination with the need for the scattered photon to subsequently undergo Compton scattering in the polarimeter detector, the lack of sufficiently intense polarized X-ray sources restricted the study of Rayleigh scattering polarization features to scenarios in which either the angular-differential scattering cross section of a linearly polarized incident beam or the polarization of the scattered radiation resulting from an unpolarized incident beam was measured.[23]

With the advent of third-generation synchrotron radiation facilities, the generation of intense, highly-polarized hard X-rays became possible reaching up to energies of a few 100 keV. More, the development of efficient Compton polarimeters, as described above, enabled highly efficient polarimetry measurements for a broad energy regime from a few 10 keV to ≈300 keV. By combining the intense radiation emitted by a third-generation synchrotron source with detection by a highly efficient Compton polarimeter in scattering experiments, the underlying theoretical models of Rayleigh scattering can be tested with unprecedented accuracy.

Utilizing the High Energy Materials Science Beamline P07[28] of the third-generation synchrotron radiation facility PETRA III at DESY and a dedicated highly efficient Compton polarimeter, it was possible for the first time to apply a highly linearly polarized incident photon source (close to 100%) for the measurements of the linear polarization of elastically scattered hard X-rays.[12] The highly linearly polarized synchrotron beam with a photon energy of $h\nu = 175$ keV was scattered on a thin gold target (see **Figure 3** for an example spectrum of such a scattering experiment).

Using the dedicated Compton polarimeter the polarization of the elastically scattered radiation was then analyzed for scattering within the polarization plane of the incident synchrotron beam. For this purpose, only the detected photons in a narrow energy window around the elastic scattering peak were analyzed. The study showed a strong depolarization of the scattered beam, which is most pronounced for scattering angles of $\theta \approx 90°$, well in accordance with theoretical predictions when including a small depolarization of the incident synchrotron beam. The exact position of the strongest depolarization of the scattered beam strongly depends on the photon energy of the incident beam and is shifted toward lower polar scattering angles for higher photon energies due to relativistic effects. The depolarization of the scattered beam under a certain polar scattering angle θ depends on the degree of linear polarization of the incident beam and the atomic target. By comparing the measured depolarization of the scattered beam under certain scattering angles with the theoretical predictions for an incident synchrotron beam with a photon energy of 175 keV being scattered on gold atoms, the degree of linear polarization of the used beamline P07 of PETRA III could be determined to be $P_{l,i} = 98\%$.

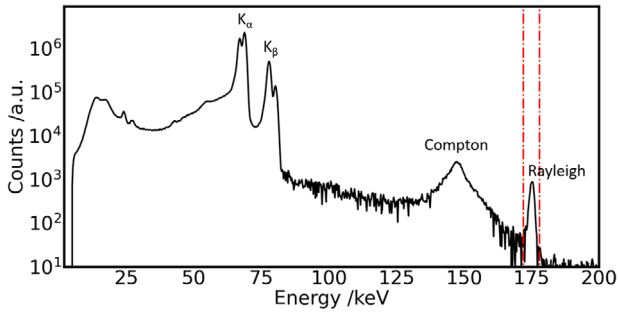

Figure 3. A typical scattering spectrum of hard X-rays with a photon energy of $h\nu = 175$ keV being scattered on gold foil measured with the dedicated Compton polarimeter under a scattering angle $\theta = 63°$. The spectrum shows the characteristic fluorescence lines K_α and K_β of the gold target, the angle-dependent Compton peak of X-rays being Compton scattered within the gold target and the Rayleigh scattering peak which has the same energy as the incident beam. Only focusing on detected photons in an energy window around the Rayleigh peak, as shown by the red dashed vertical lines, the polarization features of the elastic scattering peak can be analyzed.

For a full test of the polarization-dependent features of Rayleigh scattering one has to investigate the scattered radiation not only within the polarization plane of the incident beam but also for nonzero azimuthal scattering angles, $\varphi \neq 0°$,[24,27] since this setup enables to analyze the variation of both Stokes parameters $P_{1,f}$ and $P_{2,f}$. An experiment on Rayleigh scattering for nonzero azimuthal scattering angles was recently performed at beamline P07 of PETRA III and the data analysis is to the moment of this publication still ongoing.

At higher photon energies of $h\nu \gtrsim 1$ MeV also the other constituents of elastic scattering, in particular Delbrück scattering should be testable using this approach. So far however, due to the used detector crystal the detection efficiency of the Compton polarimeter is not sufficient above energies of 300 keV. Further upcoming improvements of the detector setup, as explained in the following chapter, will in future allow for efficient polarimetry for even higher photon energies up to the MeV range.

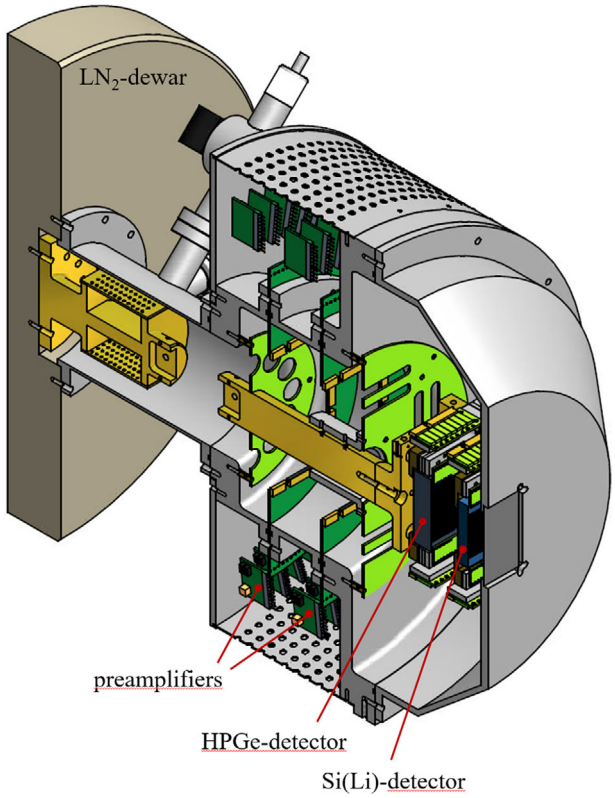

Figure 4. CAD-drawing of the planned detector setup. In front the lithium-diffused silicon detector is installed followed by a high-purity germanium crystal as stopping detector. Both detector crystals show a strip structure making them position-sensitive.

3. Possible Application of Compton Polarimetry at the Gamma Factory

3.1. Telescope Compton Polarimeter Setup with an Additional Segmented Ge-Crystal

With the described Compton polarimeter setup using a segmented silicon crystal highly efficient polarimetry measurements are possible up to around 300 keV. However for higher photon energies the detection efficiency strongly decreases due to the decreasing photoabsorption cross section of the crystal material leading to a reduced stopping power as well as due to the fact that for higher photon energies Compton scattering under forward angles becomes more and more likely. To overcome this drawback and realize a polarimeter setup for even higher photon energies in the MeV range a new detector setup was developed as can be seen in **Figure 4**. In this detector setup the already described lithium-diffused silicon detector is followed by a high-purity germanium crystal in a telescope structure. The higher nuclear charge Z of germanium leads to a higher photoabsorption cross section even for higher photon energies overcoming the drawbacks in the reduced stopping power. Similar to the silicon detector, the germanium-crystal is as well separated in a strip structure with each strip being read out separately by a cooled preamplifier. For Compton events with both the scattering of an incident photon and the absorption of the scattered photon being detected in the crystal, the same reconstruction process as described for the silicon-detector is possible.

Additionally photons being Compton scattered in the silicon detector under forward angles can be absorbed in the germanium detector. Combining the information in time, energy and position of both detectors simultaneously allows to also reconstruct such scattering events. Both the improved detection efficiency of the germanium crystal by a higher photoabsorption cross section and the combination of two crystals in a telescope structure to account for Compton scattering under forward angles will make the improved detector setup suitable for measurements at even higher photon energies which will allow polarization analysis in the MeV range.

3.2. Possible Polarization Analysis of Delbrück Scattering

First mentioned in a commentary on a publication by Lise Meitner,[22] Delbrück scattering is known today as one of the most fundamental nonlinear quantum electrodynamics (QED) processes.[29] In this process, high-energy photons are elastically scattered off the electromagnetic field of a nucleus as a consequence of the formation of virtual electron–positron pairs. In the past multiple efforts were made to observe Delbrück scattering experimentally by measurement of the cross section of elastic scattering of unpolarized high-energy photons on atoms.[30] In these studies, a good agreement between experimental results and theoretical calculations of the scattering cross section was achieved only upon theoretical account of the Delbrück component. However, for Delbrück scattering itself a conclusive experimental prove of theory is still missing. A much more sensitive test could be performed using a linear polarized photon beam as stated in Ref. [31] since for a scattering angle of 90° nuclear Thomson scattering and giant dipole resonance vanish. In their recent paper Koga and Hayakawa presented a more in depth analysis of a possible experimental scenario using a polarized γ-ray beam and measuring the differential scattering cross section for scattering within the polarization plane of the incident beam.[32] They show that the scattering cross section regarding the part of the scattered radiation being polarized in the scattering plane will be highly dominated by Delbrück scattering for certain polar scattering angles θ while the other scattering constituents are strongly suppressed. This makes an isolated measurement of the Delbrück scattering cross section feasible.

We would like to suggest an alternative approach to the precise measurement of Delbrück scattering, much similar to the studies on the polarization transfer in Rayleigh scattering, using a linearly polarized γ-ray beam. Additionally to the measurement of the scattering cross section our approach suggests the measurement of the degree of linear polarization $P_{l,f}$ and polarization angle χ of the scattered photon beam by the improved Compton polarimeter in order to determine the Stokes parameters $P_{1,f}$ and $P_{2,f}$. A possible experimental scenario would be the following: A highly linearly polarized very intense photon beam of photons in the MeV range (e.g., 1.1MeV) as can be provided by the Gamma Factory is scattered on a thin target foil (e.g., tin, Z=50, gold, Z=79 or lead, Z=82) and the scattered radiation is then detected by the Compton polarimeter.

The theoretical calculations regarding the best scattering angles and expected polarization characteristics of the scattered beam in such a scattering experiment regarding Delbrück scattering still have to be performed. For this also possible interferences occurring from the different scattering constituents have to be taken into account. However, as can already be seen for the Rayleigh scattering experiment, the simultaneous measurement of the scattering cross section and the linear polarization of the scattered beam using our Compton polarimeter, a much more stringent test of Delbrück scattering can be achieved than given solely by cross section measurements.

4. Conclusion

The 2D-sensitive Si(Li) strip detector has proven to be a valuable tool for Compton polarimetry exploiting the polarization sensitivity of Compton scattering already for photon energies up to 200 keV. By testing the polarization-dependent features of fundamental processes like Rayleigh scattering of hard X-rays, much more stringent tests of the underlying models are possible than achievable by only relying on cross section measurements. An additional installation of a segmented germanium crystal in a telescope geometry behind the already installed segmented silicon crystal will allow for the polarization analysis at even higher photon energies up to the MeV-range. In particular, these novel detector developments open a route for the polarization studies of Delbrück scattering, as can be performed at the Gamma Factory. This will allow stringent tests of the theories that describe nonlinear QED processes in the presence of extremely strong electromagnetic fields.

Acknowledgements

The authors acknowledge financial support by the German Federal Ministry for Education and Research (BMBF) under Grants No. 05P15SJFAA. W.M. acknowledges funding from BMBF via Verbundforschung 05P19SJFAA. M.V. acknowledges funding from BMBF via Verbundforschung 05P18SJRB1. Parts of this research were carried out at the light source PETRA III at DESY, a member of the Helmholtz Association (HGF).

Open access funding enabled and organized by Projekt DEAL.

Conflict of Interest

The authors declare no conflict of interest.

Data Availability Statement

Data sharing is not applicable to this article as no new data were created or analyzed in this study.

Keywords

Compton scattering, Delbrück scattering, elastic scattering, polarimetry, Rayleigh scattering

Received: June 15, 2021
Revised: November 1, 2021
Published online:

[1] J. Hough, *Astron. Geophys.* **2006**, *47*, 3.31.
[2] M. L. McConnell, J. M. Ryan, *New Astrom. Rev.* **2004**, *48*, 215.
[3] P. P. Kane, L. Kissel, R. H. Pratt, S. C. Roy, *Phys. Rep.* **1986**, *140*, 75.
[4] S. C. Roy, L. Kissel, R. H. Pratt, *Radiat. Phys. Chem.* **1999**, *56*, 3.
[5] Th. Stöhlker, D. Banaś, H. Bräuning, S. Fritzsche, S. Geyer, A. Gumberidze, S. Hagmann, S. Hess, C. Kozhuharov, A. Kumar, R. Märtin, B. E. O'Rourke, R. Reuschl, U. Spillmann, A. Surzhykov, S. Tashenov, S. Trotsenko, G. Weber, D. F. A. Winters, *Eur. Phys. J. Spec. Top.* **2009**, *169*, 5.
[6] M. Vockert, G. Weber, H. Bräuning, A. Surzhykov, C. Brandau, S. Fritzsche, S. Geyer, S. Hagmann, S. Hess, C. Kozhuharov, R. Märtin, N. Petridis, R. Hess, S. Trotsenko, Yu. A. Litvinov, J. Glorius, A. Gumberidze, M. Steck, S. Litvinov, T. Gaßner, P.-M. Hillenbrand, M. Lestinsky, F. Nolden, M. S. Sanjari, U. Popp, C. Trageser, D. F. A. Winters, U. Spillmann, T. Krings, Th. Stöhlker, *Phys. Rev. A* **2019**, *99*, 052702.
[7] R. Märtin, G. Weber, R. Barday, Y. Fritzsche, U. Spillmann, W. Chen, R. D. DuBois, J. Enders, M. Hegewald, S. Hess, A. Surzhykov, D. B. Thorn, S. Trotsenko, M. Wagner, D. F. A. Winters, V. A. Yerokhin, Th. Stöhlker, *Phys. Rev. Lett.* **2012**, *108*, 264801.
[8] A. Surzhykov, S. Fritzsche, Th. Stöhlker, S. Tashenov, *Phys. Rev. Lett.* **2005**, *94*, 203202.
[9] H. Bernhardt, B. Marx-Glowna, K. S. Schulze, B. Grabiger, J. Haber, C. Detlefs, R. Loetzsch, T. Kämpfer, R. Röhlsberger, E. Förster, Th. Stöhlker, I. Uschmann, G. G. Paulus, *Appl. Phys. Lett.* **2016**, *109*, 121106.
[10] Th. Stöhlker, V. Bagnoud, K. Blaum, A. Blazevic, A. Brauning-Demian, M. Durante, F. Herfurth, M. Lestinsky, Y. Litvinov, S. Neff, R. Pleskac, R. Schuch, S. Schippers, D. Severin, A. Tauschwitz, C. Trautmann, D. Varentsov, E. Widmann, APPA Collaborations, *Nucl. Instrum. Methods Phys. Res., Sect. B* **2015**, *365*, 680.
[11] F. Aumayr, K. Ueda, E. Sokell, S. Schippers, H. Sadeghpour, F. Merkt, T. F. Gallagher, F. B. Dunning, P. Scheier, O. Eche, T. Kirchner, S. Fritzsche, A. Surzhykov, X. W. Ma, R. Rivarola, O. Fojon, L. Tribedi, E. Lamour, J. R. C. Lopez-Urrutia, Y. A. Litvinov, V. Shabaev, H. Cederquist, H. Zettergren, M. Schleberger, R. A. Wilhelm, T. Azuma, P. Boduch, H. T. Schmidt, T. Stöhlker, *J. Phys. B: At., Mol. Opt. Phys.* **2019**, *52*, 171003.
[12] K.-H. Blumenhagen, S. Fritzsche, T. Gassner, A. Gumberidze, R. Märtin, N. Schell, D. Seipt, U. Spillmann, A. Surzhykov, S. Trotsenko, *New J. Phys.* **2016**, *18*, 103034.
[13] G. Weber, H. Bräuning, A. Surzhykov, C. Brandau, S. Fritzsche, S. Geyer, S. Hagmann, S. Hess, C. Kozhuharov, R. Märtin, N. Petridis, R. Reuschl, U. Spillmann, S. Trotsenko, D. F. A. Winters, Th. Stöhlker, *Phys. Rev. Lett.* **2010**, *105*, 243002.
[14] M. Vockert, G. Weber, U. Spillmann, T. Krings, M. O. Herdrich, Th. Stöhlker, *Nucl. Instrum. Methods Phys. Res., Sect. B* **2017**, *408*, 313.
[15] F. Metzger, M. Deutsch, *Phys. Rev.* **1950**, *78*, 551.
[16] F. Lei, A. J. Dean, G. L. Hills, *Space Sci. Rev.* **1997**, *82*, 309.
[17] G. Weber, H. Bräuning, A. Surzhykov, C. Brandau, S. Fritzsche, S. Geyer, R. E. Grisenti, S. Hagmann, C. Hahn, R. Hess, C. Kozhuharov, M. Kühnel, R. Märtin, N. Petridis, U. Spillmann, S. Trotsenko, D. F. A. Winters, Th. Stöhlker, *J. Phys. B: At., Mol. Opt. Phys.* **2015**, *48*, 144031.
[18] M Vockert, G Weber, U Spillmann, T Krings, Th Stöhlker, *J. Phys.: Conf. Ser.* **2018**, *1024*, 012041.
[19] W. Franz, *Z. Phys.* **1935**, *98*, 314.
[20] Z. Berant, R. Moreh, S. Kahane, *Phys. Lett. B* **1977**, *69*, 281.
[21] E. G. Fuller, E. Hayward, *Nucl. Phys.* **1962**, *30*, 613.
[22] L. Meitner, H. Kösters, *Z. Phys.* **1933**, *84*, 137.
[23] S. C. Roy, B. Sarkar, L. D. Kissel, R. H. Pratt, *Phys. Rev. A* **1986**, *34*, 1178.
[24] S. Strnat, V. A. Yerokhin, A. V. Volotka, G. Weber, S. Fritzsche, R. A. Müller, A. Surzhykov, *Phys. Rev. A* **2021**, *103*, 012801.
[25] A. Surzhykov, V. A. Yerokhin, T. Jahrsetz, P. Amaro, Th. Stöhlker, *Phys. Rev. A* **2013**, *8898*, 062515.

[26] A. Surzhykov, V. A. Yerokhin, Th. Stöhlker, S. Fritzsche, *J. Phys. B: At., Mol. Opt. Phys.* **2015**, *48*, 144015.
[27] A. V. Volotka, A. Surzhykov, S. Fritzsche, *Phys. Rev. A* **2020**, *102*, 042814.
[28] N. Schell, A. King, F. Beckmann, T. Fischer, M. Müller, A. Schreyer, *Mater. Sci. Forum* **2013**, *772*, 57.
[29] V. Costantini, B. De Tollis, G. Pistoni, *Nuovo Cimento Soc. Ital. Fis.* **1971**, *A2*, 733.
[30] M. Schumacher, *Radiat. Phys. Chem.* **1999**, *56*, 101.
[31] B. De Tollis, G. Pistoni, *Nuovo Cimento Soc. Ital. Fis.* **1977**, *A42*, 499.
[32] J. K. Koga, T. Hayakawa, *Phys. Rev. Lett.* **2017**, *118*, 204801.